BMC Medical Genomics

RESEARCH

Open Access

Transcriptome-wide N6-methyladenosine modification profiling of long non-coding RNAs in patients with recurrent implantation failure

Ting Wang[1†], Lili Zhang[2,3†], Wenxin Gao[5†], Yidan Liu[4], Feng Yue[2,3], Xiaoling Ma[2,3] and Lin Liu[1,2,3,4*]

Abstract

N^6-methyladenosine (m^{6}A) is involved in most biological processes and actively participates in the regulation of reproduction. According to recent research, long non-coding RNAs (lncRNAs) and their m^{6}A modifications are involved in reproductive diseases. In the present study, using m^{6}A-modified RNA immunoprecipitation sequencing (m^{6}A-seq), we established the m^{6}A methylation transcription profiles in patients with recurrent implantation failure (RIF) for the first time. There were 1443 significantly upregulated m^{6}A peaks and 425 significantly downregulated m^{6}A peaks in RIF. Gene Ontology and Kyoto Encyclopedia of Genes and Genomes pathway analyses revealed that genes associated with differentially methylated lncRNAs are involved in the p53 signalling pathway and amino acid metabolism. The competing endogenous RNA network revealed a regulatory relationship between lncRNAs, microRNAs and messenger RNAs. We verified the m^{6}A methylation abundances of lncRNAs by using m^{6}A-RNA immunoprecipitation (MeRIP)–real-time polymerase chain reaction. This study lays a foundation for further exploration of the potential role of m^{6}A modification in the pathogenesis of RIF.

Keywords Recurrent implantation failure, N6-methyladenosine, M^{6}A modified RNA immunoprecipitation sequencing, Long non-coding RNAs

Background

The success rate of assisted reproductive technology exceeds 50%, but some patients fail after recurrent implantation, which leads to large financial and psychological burdens. Recurrent implantation failure (RIF) is usually defined as a failure to achieve clinical pregnancy after at least four high-quality embryos are transferred in women under the age of 40 years within at least three fresh or frozen cycles [1]. Low endometrial receptivity is considered to be the main cause of RIF [2]. During a normal menstrual cycle, 6–8 days after ovulation is considered to be the window of implantation when endometrial receptivity is highest [3]. At this time, pinopodes, which are membranous protuberances, can be observed under a scanning electron microscope; they are considered to be a morphological marker of endometrial receptivity [4]. There are several molecular change that are associated with endometrial receptivity, have been detected in women with RIF, including mucin 1, integrin β3, homeobox A10 and leukaemia inhibitor factor (*LIF*)

†Ting Wang, Lili Zhang and Wenxin Gao contributed equally to this work.

*Correspondence:
Lin Liu
ldyy_liul@lzu.edu.cn
[1] The First Clinical Medical College of Lanzhou University, Lanzhou University, Lanzhou, Gansu, China
[2] The Reproductive Center, The First Hospital of Lanzhou University, Lanzhou, Gansu, China
[3] Clinical Research Center for Reproductive Diseases of Gansu Province, Lanzhou, Gansu, China
[4] The Basic Medical Sciences College of Lanzhou University, Lanzhou, Gansu, China
[5] School of Nursing, Shaanxi University of Chinese Medicine, Xianyang, Shaanxi, People's Republic of China

[5–7]. However, the precise aetiology and pathogenesis of RIF remains unclear.

N^6-methyladenosine (m^{6}A) was first discovered in 1974. It is the most common RNA modification in eukaryotes [8]. Researchers have confirmed that the formation, removal and other functions of m^{6}A are accomplished by three types of regulatory proteins [9]. m^{6}A modification is catalysed by the methyltransferase 'writer' complex that comprises methyltransferase-like 3 (*METTL3*); methyltransferase-like 14 (*METTL14*); Wilms' tumour 1-associating protein (*WTAP*); and other proteins with methyltransferase capability, including RNA-binding motif protein 15 (*RBM15*) and zinc finger CCCH-type containing 13 (*ZC3H13*) [10]. The demethylase complex includes ALKB homolog 5 (*ALKBH5*) and fat mass and obesity associated gene (*FTO*); it removes m^{6}A, thus acting as an 'eraser'. Finally, m^{6}A-modified RNA can be recognised and regulated by m^{6}A-binding protein complexes, including YTH domain family proteins 1–3 (*YTHDF1–3*), and other proteins, which acting as 'readers' [11]. A 2021 study confirmed downregulated *METTL16* and *WTAP* messenger RNA (mRNA) levels and upregulated *ALKBH5* and *IGF2BP2* mRNA levels in the endometrium of patients with infertility [12]. Of note, it has been proved that global m^{6}A methylation and *METTL3* expression are significantly increased in the endometrial tissues from women with RIF [13]. This evidence indicates that m^{6}A modification is critical in the endometrium of patients with RIF.

Long noncoding RNAs (lncRNAs) are a class of noncoding RNAs that are longer than 200 nucleotides (nt). For a long time, they were regarded as transcriptional noise because of their low expression and non-protein coding features. Recently, lncRNAs have been indicated to play an important role in embryo implantation. For example, *TUNAR* might participate in embryo implantation by regulating the adhesion of blastocysts to endometrial epithelium and the proliferation and decidualisation of endometrial stromal cells (ESCs) [14]. *CECR3* and five other lncRNAs together with their competing endogenous RNA (ceRNA) sub-networks, might be involved in immunological activity, growth factor binding, vascular proliferation, apoptosis, steroid biosynthesis in the uterus and preparing endometrium for embryo implantation [15]. Therefore, the regulation mediated by lncRNAs may affect embryo implantation. In addition, researchers have demonstrated that lncRNAs present abundant m^{6}A methylation [16, 17]. The m^{6}A-modified lncRNA profile has been established in many diseases, including coronary artery disease [18], gastric cancer [19], ameloblastoma [20] and systemic lupus erythematosus [21]. Recently, m^{6}A-modified lncRNAs have been shown to inhibit human trophoblast cell proliferation and to induce miscarriage [22]. However, the m^{6}A-modified lncRNA methylome in patients with RIF has not yet been determined.

In this study, we used m^{6}A-modified RNA immunoprecipitation sequencing (m^{6}A-seq) to establish the m^{6}A-methylation transcription profiles in RIF for the first time. We identified differentially methylated peaks and then constructed a ceRNA was constructed by using bioinformatics to reveal a regulatory relationship between lncRNAs, microRNAs (miRNAs) and mRNAs. Our findings provide new insights into the pathogenic mechanism of RIF.

Materials and methods

Patients and tissue samples

This study was approved by the Ethics Committee of First Hospital of Lanzhou University (No: LDYYLL2019-45). The participants were recruited from the First Hospital of Lanzhou University. The inclusion criteria were (1) < 40 years old; (2) a regular menstrual cycle (25–35 days); and (3) normal basal serum sex hormone levels, namely < 10 mIU/mL for follicle-stimulating hormone (FSH), < 10 mIU/mL for luteinising hormone (LH) and < 50 pg/mL for oestradiol (ES), measured on days 2–3 of the menstrual cycle. The exclusion criteria were: (1) chromosomal anomaly based on a peripheral blood test; (2) tested positive for anticardiolipin antibody or lupus anticoagulant; (3) polycystic ovary syndrome (PCOS); (4) uterine anomalies (congenital uterine anomaly, fibroid, polyps and intrauterine adhesions); (5) abnormal blood glucose level or thyroid dysfunction function test; and/or (6) use steroid hormone in the preceding 2 months. According to the RIF definition, women with RIF had failed to achieve clinical pregnancy after at least four high-quality embryos had been transferred for a minimum of three cycles [1]. The control participants, who became pregnant during the cycle after sampling, underwent IVF/ICSI-ET due to fallopian tube or male factors.

Six women were recruited for this study: three for the RIF group and three for the control group. Endometrial samples were obtained on day LH + 7 via pipe suction curettage, placed in cryopreservation tubes and stored at − 80°C. These samples were from the middle secretory phase, as confirmed by histology.

RNA extraction and quality control

Total RNA was isolated from the endometrial samples with the TRIzol Reagent (Invitrogen, Gibco-BRL, Bethesda, MD, USA) according to the manufacturer's instructions. A NanoDropND-1000 was utilised to determine the RNA concentration; the 260/280 ratio was 1.8–2.1. The quality of the RNA was assessed based on

Table 1 Primer sequences used for RT-qPCR

transcript_id	Primer sequences (5′-3′)	
	Forward	Reverse
ENST00000416361	GGGGAAATGTGGGGAAAAGA	GATCAACAGCATCCCAAGGC
ENST00000471664	AGTGACTCTTCTTGGACCAGG	ATTGTGCCTCTCCAATCTGC

the 18S/28S ribosomal RNA (rRNA) band intensity in 1% agarose gels containing ethidium bromide. In addition, following the immunoprecipitation, a 2100 Bioanalyzer (Agilent) was used to assess the RNA quality.

Preparation and sequencing of the RNA and MeRIP libraries

The m^{6}A-Seq service was provided by CloudSeq Inc. (Shanghai, China). In accordance with manufacturer's instructions, total RNA was immunoprecipitated using the m^{6}A-IP Kit (GenSeq Inc.). In brief, RNA was randomly fragmented to about 200 nt using the RNA Fragmentation Reagent, and Protein A/G beads were rotated for 1 h to couple protein to antibody. Bead-linked antibodies were incubated with RNA fragments for 4 h at 4 °C. After incubation, the RNA/antibody complexes were washed several times. Then, captured RNA was eluted from the complexes and purified. The RNA libraries for the IP and input samples were constructed using the Low Input Whole RNA Library Prep Kit (GenSeq), following the manufacturer's instructions. After evaluating the quality of the libraries with a 2100 bioanalyzer (Agilent), sequencing was carried out on a NovaSeq instrument (Illumina).

RNA-seq

High-throughput RNA-seq was performed by CloudSeq Biotech. Briefly, rRNA was removed from total RNA with the rRNA Removal Kit (GenSeq, Inc.). Then, the rRNA-depleted samples were used to construct libraries with the Low Input RNA Library Prep Kit (GenSeq, Inc.) according to the manufacturer's instructions. The library quality and quantity were analysed using a 2100 BioAnalyzer (Agilent). The libraries were sequenced with a Novaseq 6000 sequencer (Illumina) with 150 base pair (bp) paired-end reads.

MeRIP-real-time polymerase chain reaction (qPCR)

Three differentially expressed genes with differentially methylated m^{6}A peaks were used for MeRIP-qPCR validation. RNA was extracted and quantified as described above. A small proportion of fragmented RNA was used as the input control. The remaining RNA was incubated with magnetic beads coupled with an m^{6}A antibody. Then, m^{6}A RNA was eluted from the magnetic beads, according to the manufacturer's instructions. The m^{6}A IP samples and input samples were collected for reverse transcription (RT)-qPCR. The primers for MeRIP-qPCR are shown in Table 1.

Data analysis

Briefly, the Novaseq 6000 reads were subjected to quality control with Q30 [23]. After 3′ adaptor-trimming and removing low-quality reads with the cutadapt software (v1.9.3), the high-quality trimmed reads were used to analyse lncRNAs and mRNAs. They were aligned to the reference genome (UCSC hg19) with the hisat2 software (v2.0.4) [24]. Then, the HTSeq software (v0.9.1) [25] was used to obtain the gene level (mRNA) and transcript level (lncRNA) raw counts, and edgeR (v3.16.5) [26] was used for normalisation. Differentially expressed mRNAs were identified based on the p-value and fold change. Gene Ontology (GO) analysis and Kyoto Encyclopedia of Genes and Genomes (KEGG) analyses were performed based on the differentially expressed mRNAs. Methylated sites on RNAs were identified with the MACS software [27]. Differentially methylated sites were identified using diffReps [28]. The lncRNA target genes were predicted, and GO and KEGG analyses were performed based on these target genes [29].The miRNA-target gene prediction software programs lncRNASNP2 [30] and TargetScan [31] were used to predict miRNAs and mRNAs, which were combined for the screened lncRNAs. The ceRNA network was plotted using Cytoscape (v3.9.1) [32].

(See figure on next page.)

Fig. 1 The characteristics of m^{6}A methylation in RIF. **A** A Venn diagram of m^{6}A modification sites identified in lncRNAs from the RIF group (green) and the control group (blue). **B** A Venn diagram of m^{6}A-modified lncRNAs from the RIF group (green) and the control group (blue). **C** The general number of differentially methylated peaks and associated lncRNAs; orange and blue represent hypermethylated and hypomethylated lncRNAs, respectively. **D** Cluster analysis of the m^{6}A-modified lncRNA genes in the RIF and control groups. Red and green represent up- and downregulated peaks, respectively (fold-change ≥ 2.0, $P < 0.00001$). **E** The top five m^{6}A motifs enriched in the RIF and control groups

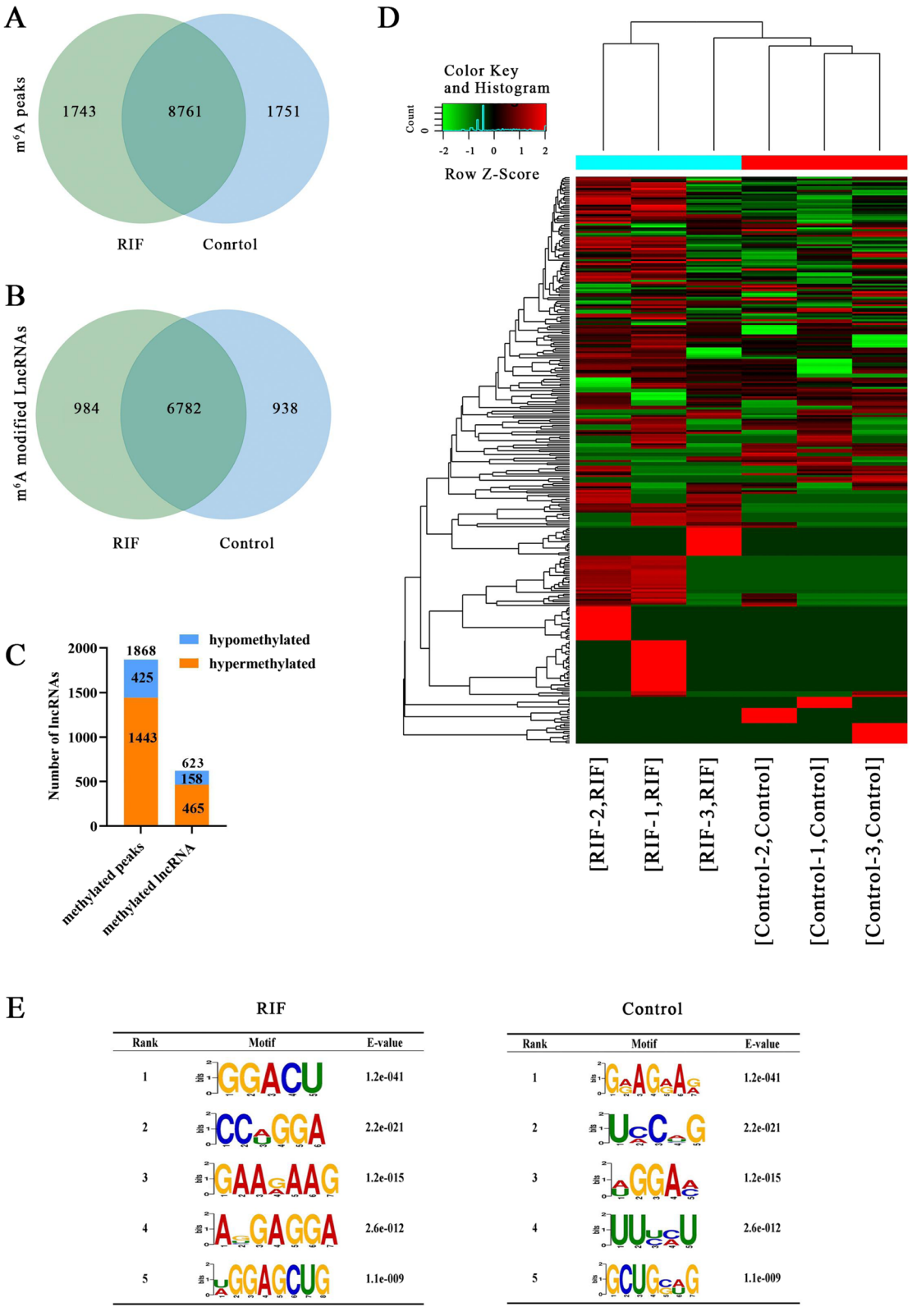

Fig. 1 (See legend on previous page.)

Table 2 Top ten hypermethylated lncRNAs

Chromosome	txStart	txEnd	transcript_id	GeneName	Foldchange
chr2	3688901	3689022	NR_045659	COLEC11	96.7
chr2	219256098	219256280	ENST00000490872	SLC11A1	93.8
chr17	18394001	18394380	ENST00000584127	LGALS9C	75.5
chr17	72599881	72600260	ENST00000569279	CTD-2006K23.1	75.4
chr12	10365056	10365220	ENST00000539408	GABARAPL1	73.3
chr19	11908261	11908500	ENST00000589227	CTC-499B15.7	73.1
chr3	183240361	183240924	ENST00000487643	KLHL6	72.3
chr2	233215941	233216019	ENST00000427961	ECEL1P3	71.2
chr19	47235821	47235957	ENST00000600716	CTB-174O21.2	67.9
chr2	166933597	166933662	ENST00000599041	AC010127.3	67.0

Results

Characteristics of m^{6}A methylation in patients with RIF

We performed genome-wide profiling of m^{6}A-modified lncRNAs in three control participants and three patients with RIF group. We have submitted the data to the Gene Expression Omnibus (GEO accession number GSE205398). We identified 10,504 and 10,512 m^{6}A peaks in the RIF and control groups, respectively. Of these peaks, 8761 were common to both the RIF and control groups, 1743 were unique to the RIF group and 1751 were unique to the control group (Fig. 1A). As shown in Fig. 1B, the 10,504 m^{6}A peaks in the RIF group were mapped to 7766 lncRNAs, and the 10,512 m^{6}A peaks in the control group were mapped to 7720 lncRNAs in the control group. Of these lncRNAs, 6782 were common to the RIF and control groups, 984 were unique to the RIF group and 938 were unique to the control group. Among the 8761 common peaks, there were 1868 significantly differentially methylated peaks (fold change ≥ 2 and $P \leq 0.0001$). The 1868 differentially methylated m^{6}A peaks were located across 623 lncRNAs. Among these lncRNAs, 158 were hypomethylated and 465 were hypermethylated (Fig. 1C). All methylated lncRNAs were clustered (fold-change ≥ 2.0 and $P \leq 0.00001$), indicating differential expression between the RIF and control groups (Fig. 1D). We searched for motifs that were enriched in the 50-bp area around m^{6}A peak by DREME software [33]. As shown in Fig. 1E, the identified m^{6}A peaks contain a conserved RRACH motif, where R represents purine, A is m^{6}A and H is a non-guanine base). This finding suggests the existence of m^{6}A methylation mechanism.

Distribution of differentially methylated m^{6}A peaks

As shown in Fig. 2A, compared with the control group, there were 1443 significantly upregulated m^{6}A peaks and 425 significantly downregulated m^{6}A peaks in the RIF group (fold change ≥ 2 and $P \leq 0.0001$). They are listed in Supplementary Table 1. The top 10 hypermethylated lncRNAs and hypomethylated lncRNAs are listed in Tables 2 and 3, respectively. We divided the m^{6}A-modified lncRNAs into six categories based on the positional relationship between the m^{6}A methylated lncRNA and mRNA: bidirectional, exon sense overlap, intron sense overlap, intron antisense, natural antisense and intergenic [34]. We found that 51.02% of the differentially m^{6}A-methylated lncRNAs were in the

Table 3 Top ten hypomethylated lncRNAs

Chromosome	txStart	txEnd	transcript_id	GeneName	Foldchange
chr22	17155996	17156936	ENST00000338526	ANKRD62P1-PARP4P3	169.3
chr14	90314776	90314840	ENST00000550103	EFCAB11	140.1
chr9	80864161	80864460	ENST00000536374	CEP78	112.9
chr7	101032148	101032361	ENST00000413033	RP5-1106H14.1	108
chr9	21395981	21396345	ENST00000569618	RP11-354P17.15	102.7
chr3	77679221	77679620	ENST00000470802	ROBO2	100.1
chr8	104029261	104029817	ENST00000518264	NPM1P52	97
chr1	71927243	71927500	ENST00000587066	ZRANB2-AS2	89.8
chr13	78233547	78233560	ENST00000450718	SPTLC1P5	87.6
chr6	27235891	27236080	ENST00000604325	XXbac-BPGBPG24O18.1	85

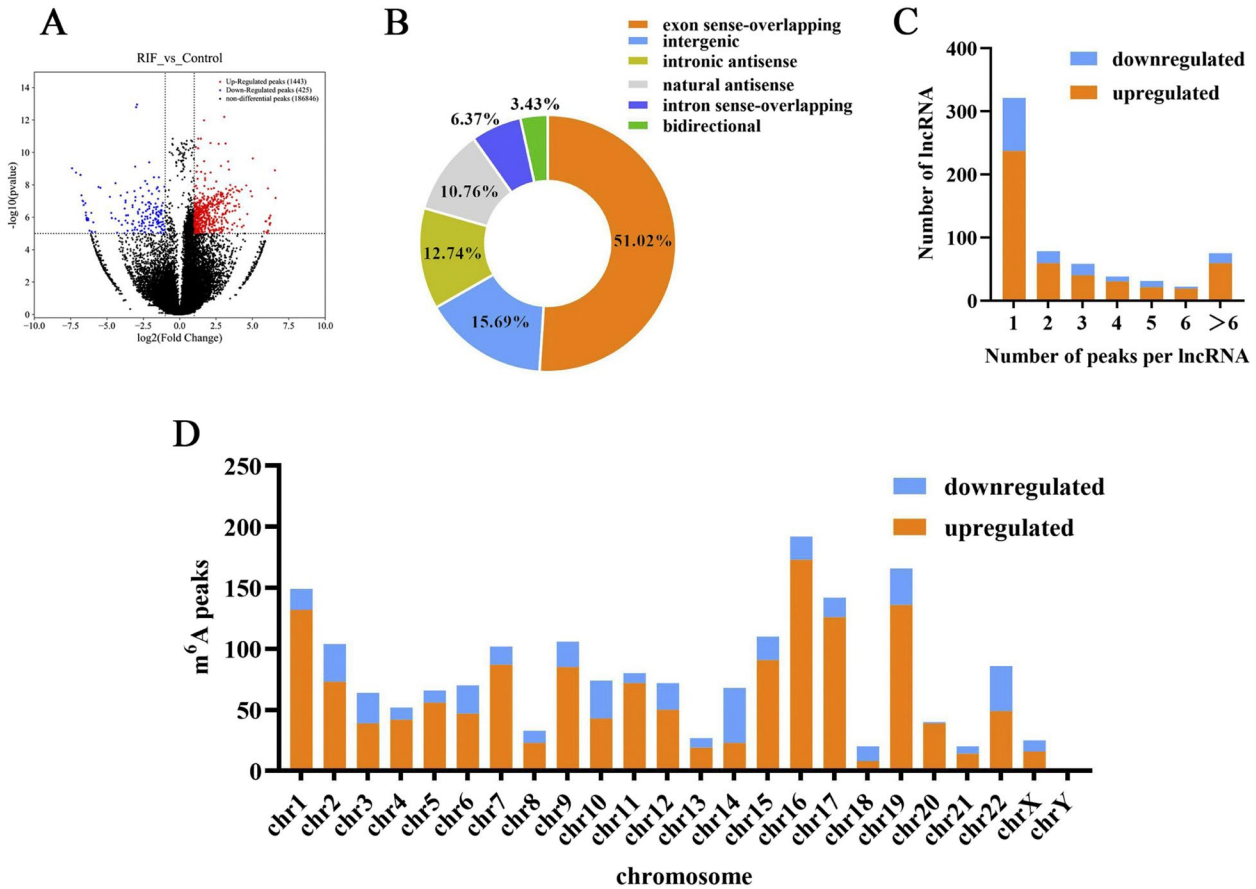

Fig. 2 Distribution of differentially methylated m^{6}A sites. **A** The volcano plot indicates the distribution of differential m^{6}A peaks the in RIF. Red and blue represent up- and downregulated peaks, respectively (fold-change ≥ 2.0, $P < 0.00001$ with Fisher's exact test). **B** The positional relationship between differentially m^{6}A methylated lncRNAs and mRNAs. Orange, DodgerBlue, olive, light grey, blue and green represent exon sense-overlap, intergenic, intronic antisense, natural antisense, intron sense-overlap and bidirectional, respectively. **C** The distribution of altered m^{6}A peaks per lncRNA. Blue and orange represent down- and upregulated peaks, respectively. **D** The chromosomal distribution of all differentially methylated sites within lncRNAs. Blue and orange represent down- and upregulated peaks, respectively

exon sense overlap group (Fig. 2B). We found that the majority of lncRNAs had one m^{6}A peak. We explored the global role of m^{6}A modification on the regulation of gene expression, especially the distribution pattern on different chromosomes (Fig. 2D). The differentially m^{6}A-methylated peaks could be mapped to all chromosomes, except the Y chromosome; chromosomes 1, 16 and 19 were particularly well represented. These results suggest that chromosomal specificity regarding m^{6}A modification could regulate the complexity of gene expression and contribute to RIF.

Differentially methylated lncRNAs are involved in the phospholipase D (PLD) and p53 signalling pathways

We explored the physiological and pathological significance of m^{6}A modification in patients with RIF by performing GO and KEGG pathway analyses for the genes associated with differentially methylated lncRNA. For GO analysis, we determined the top 10 significantly enriched genes associated with hyper- and hypomethylated lncRNAs related to biological processes, cellular components and molecular functions. The genes associated with hypermethylated lncRNAs are significantly enriched in neuron projection, regulation of GTPase activity and nucleoside-triphosphatase regulator activity (Fig. 3A). The genes associated with hypomethylated lncRNAs are significantly enriched in regulation of chromosome segregation, the Golgi stack, and peptidase activity (Fig. 3B). For KEGG pathway analysis, we found that the genes associated with hypermethylated lncRNAs in patients with RIF are significantly associated with choline metabolism; the PLD signalling pathway; and valine, leucine and isoleucine degradation (Fig. 3C). The genes associated with hypomethylated lncRNAs are involved in the p53 signalling pathway, transcriptional misregulation in cancer and natural killer (NK) cell–mediated

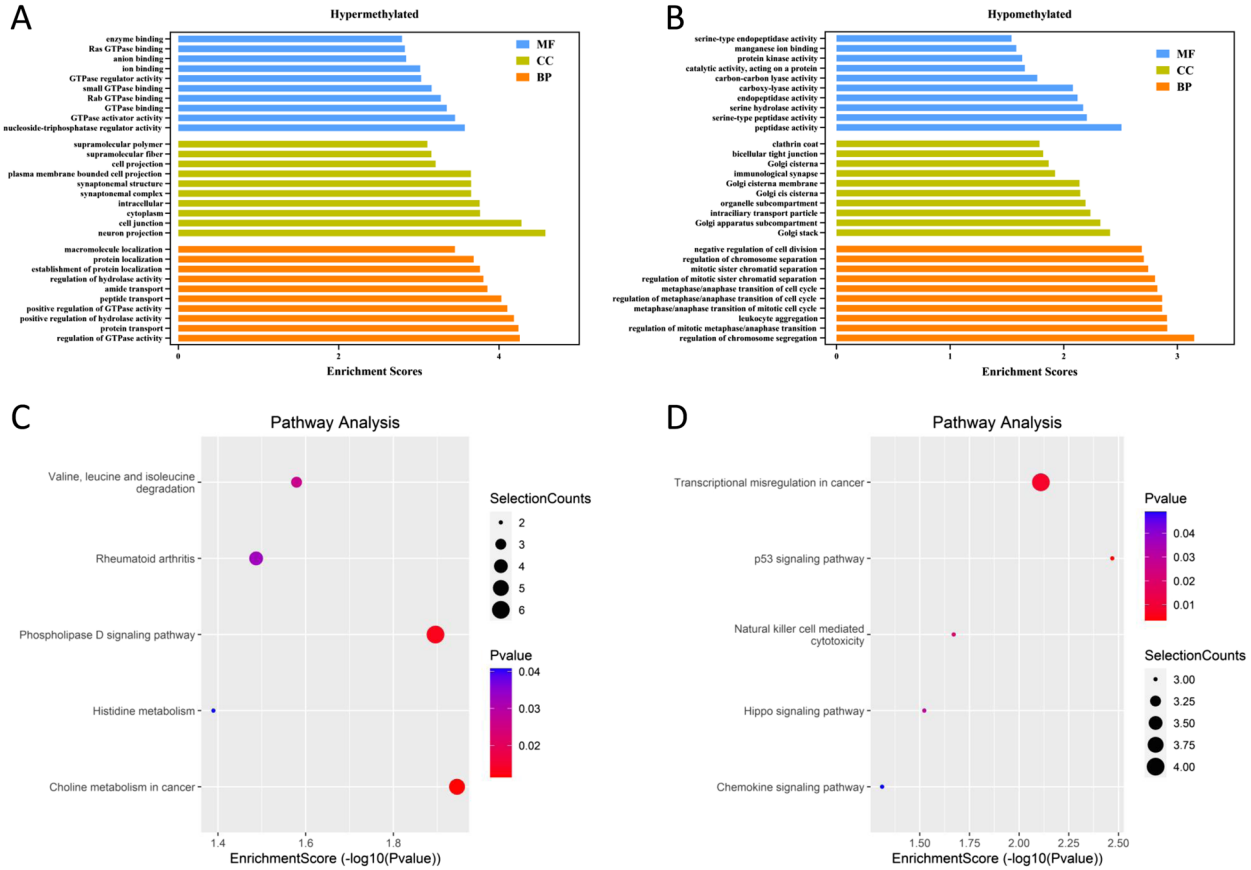

Fig. 3 **A** and **B** The top 10 GO terms for genes associated with hyper- and hypomethylated lncRNAs, respectively. Orange indicates biological process, green indicates molecular function and blue indicates cellular component. **C** and **D** The top 5 KEGG pathways of genes associated with hyper- and hypomethylated lncRNAs, respectively

cytotoxicity (Fig. 3D). We found that the PLD (Fig. 4A) and p53 (Fig. 4B) signalling pathways [35] are the most significant enriched pathways.

Construction of a lncRNA–miRNA–mRNA network for RIF

To explore the mRNAs regulated by lncRNAs, we screened 5 of 454 hypermethylated lncRNAs with a fold-change > 70 and 5 of 151 hypomethylated lncRNAs with a fold-change > 60 (Table 4). We constructed a ceRNA network based on lncRNA–miRNA–mRNA association analysis (Fig. 5). The network consists of the top five miRNAs (defined by exact probability from lncRNASNP2) combined with a screened lncRNA and the top five mRNAs (defined by the cumulative weighted context + + score) bound to the miRNAs, including 10 lncRNAs, 49 miRNAs and 232 mRNAs (Supplementary Table 2). From this ceRNA network, it is clear that lncRNAs regulate miRNAs and mRNAs. In a previous study, the authors showed that lncRNAs could act as an miRNA sponge to interact with miR-548 s and increase *ALDH1A3* mRNA expression. This action promotes glucose metabolism and cell proliferation in hepatocellular carcinoma [36]. We speculate that *LINC01152* could act as a sponge for hsa-miR-6801-3p to affect *LIF* expression.

Verification of differential lncRNA m^{6}A methylation and expression

We evaluated the association between the expression of lncRNA and m^{6}A methylation by conducting a conjoint analysis of the m^{6}A-seq and RNA-Seq data. We identified 72 lncRNAs (Supplementary Table 3) with differential m^{6}A methylation and expression levels (Fig. 6C). We divided these genes into four categories: 27 hypermethylated and self-regulated lncRNAs, 19 hypermethylated and self-downregulated lncRNAs, 33 hypomethylated and self-downregulated lncRNAs and 1 hypomethylated and self-upregulated lncRNA. Among the 72 lncRNA in Supplementary Table 3, we randomly selected two (ENST00000416361 and ENST00000471664). We determined their m^{6}A methylation abundance using the Integrative Genomics Viewer (IGV) (Fig. 6A, B) and validated

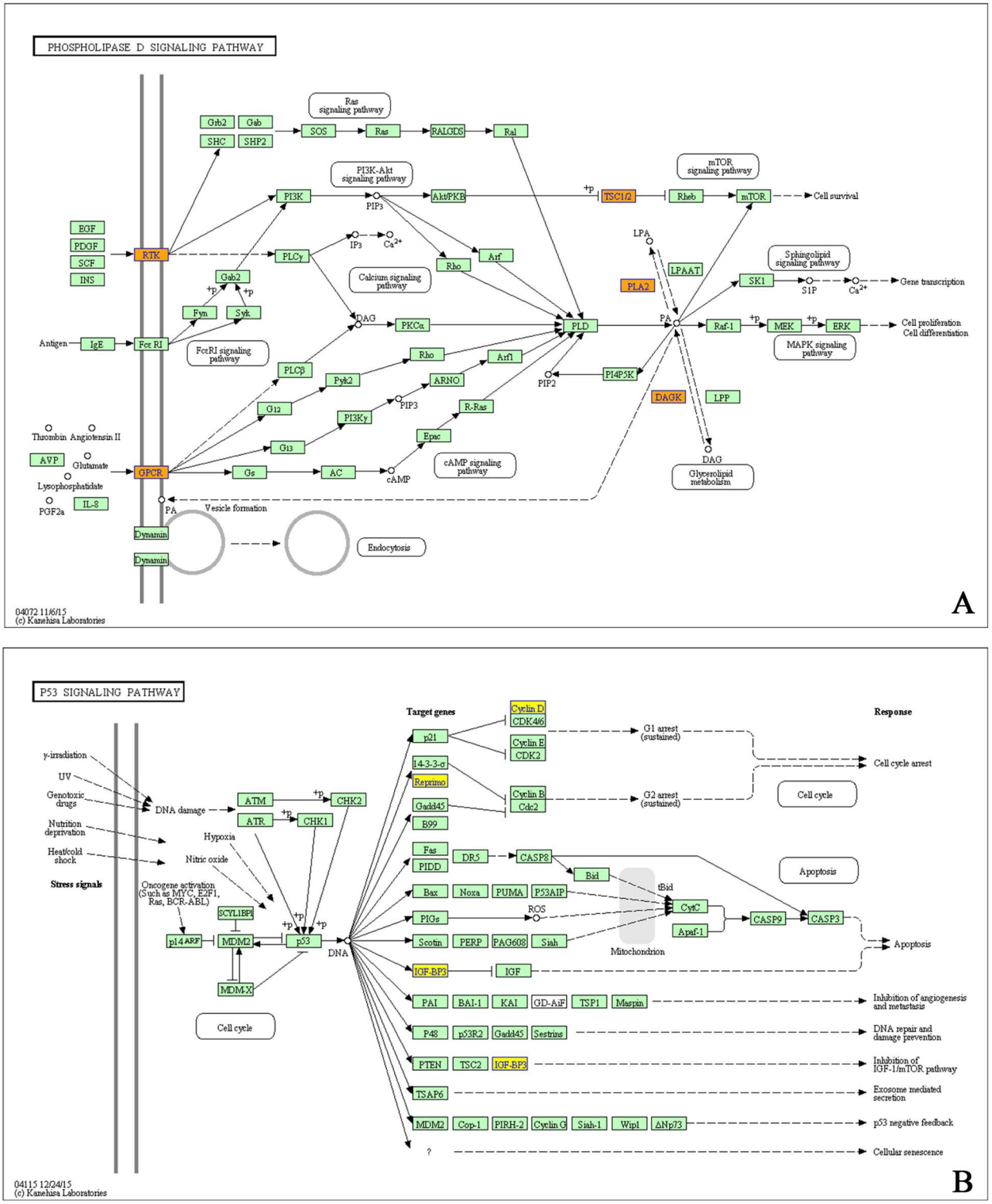

Fig. 4 Diagrams of the (**A**) phospholipase D and (**B**) p53 signalling pathways. These images have been reproduced from a previous publication [35] according to an open access licence

Table 4 LncRNAs screened for lncRNA-miRNA-mRNA analysis

transcript_id	GeneName	Foldchange	Regulation
NR_045659	COLEC11	96.7	hypermethylate
ENST00000490872	SLC11A1	93.8	hypermethylate
ENST00000539408	GABARAPL1	73.3	hypermethylate
ENST00000487643	KLHL6	72.3	hypermethylate
ENST00000599041	AC010127.3	67.0	hypermethylate
ENST00000550103	EFCAB11	140.1	hypomethylate
ENST00000536374	CEP78	112.9	hypomethylate
ENST00000413033	RP5-1106H14.1	108	hypomethylate
ENST00000569811	GOLGA8B	78.1	hypomethylate
ENST00000538693	LINC01152	73.5	hypomethylate

the findings with MeRIP-qPCR (Fig. 7A, B). Finally, RT-qPCR revealed that the relative mRNA expression of ENST00000416361 and ENST00000471664 in endometrial tissue from the RIF group and Control group. was consistent with the sequencing results (Fig. 7C, D).

Discussion

RIF is a challenging clinical dilemma. m^6A modifications play a vital role in reproductive diseases, but prior to our study, the m^6A-modified lncRNA profile of RIF had not been characterised. We established the transcriptome-wide lncRNA m^6A modification profile in RIF by using m^6A-Seq. We identified 1868 differentially methylated lncRNA m^6A peaks in endometrial tissue from patients with RIF, including 1443 significantly upregulated m^6A peaks and 425 significantly downregulated m^6A peaks. Furthermore, we explored differential expression patterns of differentially methylated lncRNAs as well as GO and KEGG pathway analyses to reveal the potential functions of differentially methylated transcripts. We also constructed a ceRNA network to reveal the regulatory relationships between lncRNAs, miRNAs and mRNAs. Our findings provides insights regarding the directions for the diagnosis and treatment of RIF in the future.

m^6A plays a crucial role in human fertility. As early as 2013, researchers identified that *ALKBH5*, a genes that encodes an m^6A 'eraser', impairs fertility by affecting apoptosis of spermatocytes in meiotic metaphase [37]. Subsequently, several m^6A regulators have been discovered to play an important role in reproductive diseases, such as endometriosis [38], polycystic ovary syndrome [39] and primary ovarian insufficiency [40]. In one study, the authors used a colourimetric m^6A quantification strategy to examine the m^6A level in control subjects and patients with RIF [13]. They found a significantly increased global m^6A level in endometrial tissues from patients with RIF compared with the controls. This finding consistent with our study (Fig. 1D) and indicates that m^6A is important for the pathogenesis of RIF.

Non-coding RNAs are important in RIF. The HOX family members are critical regulators in endometrial decidualisation [41]. In patients with RIF, *HOXA11-AS*, a lncRNA in the HOX gene family, is elevated and there is impaired *PKM2* splicing [42]. *LINC02190* is upregulated in the endometrium of patients with RIF and decreases the adhesion rate of Ishikawa and JAR cells [43]. Given the abundant published evidence, the role of lncRNAs in RIF cannot be ignored. Consistently, our study has provided novel findings regarding m^6A modified of lncRNA in RIF.

As shown in Fig. 2B, most differentially m^6A-modified lncRNAs are exon sense overlap. In a previous study, the authors found that the majority of differentially m^6A-modified lncRNAs in colorectal cancer are also exon sense overlap [44]. However, there have been different findings from other studies. Most differentially methylated m^6A sites within lncRNAs are located in intergenic region in coronary artery disease [18] and gastric cancer [19]. Thus, the dominant category of m^6A-modified lncRNAs can differ depending on the disease. Of note, exon sense overlap lncRNAs are relevant to cell proliferation, invasion and metastasis, and thus the differentially m^6A-modified exon sense overlap mRNAs we identified may play in RIF.

We found that the differentially methylated lncRNAs are related to several important biological pathways, especially choline metabolism, the PLD signalling pathway and amino acid metabolism. Choline metabolism is related to the PLD signalling pathway. PLD hydrolyses phosphatidylcholine into phosphatidic acid, a lipid signalling molecule, and choline [45], a micronutrient and a methyl donor [46]. Arzu Yurci et al. [47] reported lower choline levels in patients with RIF compared with individuals with normal fertility based on magnetic resonance spectroscopy. These results suggest that choline may participate in the pathogenesis of RIF through m^6A methylation. Moreover, genes associated with hypermethylated lncRNAs are related to the metabolism of amino acids such as valine and histidine. Increasing evidence has demonstrated that amino acid metabolism is a key regulator in RIF. In previous studies, researchers found that valine is significantly downregulated in women with repeated implantation success compared with women with RIF [48]. In a recent systematic review, the authors found that alanine, aspartate and glutamate metabolism has the greatest impact on RIF [49]. Based on our results, we suggest that m^6A methylation influences the outcome of embryo implantation via altered valine and histidine metabolism. A previous study

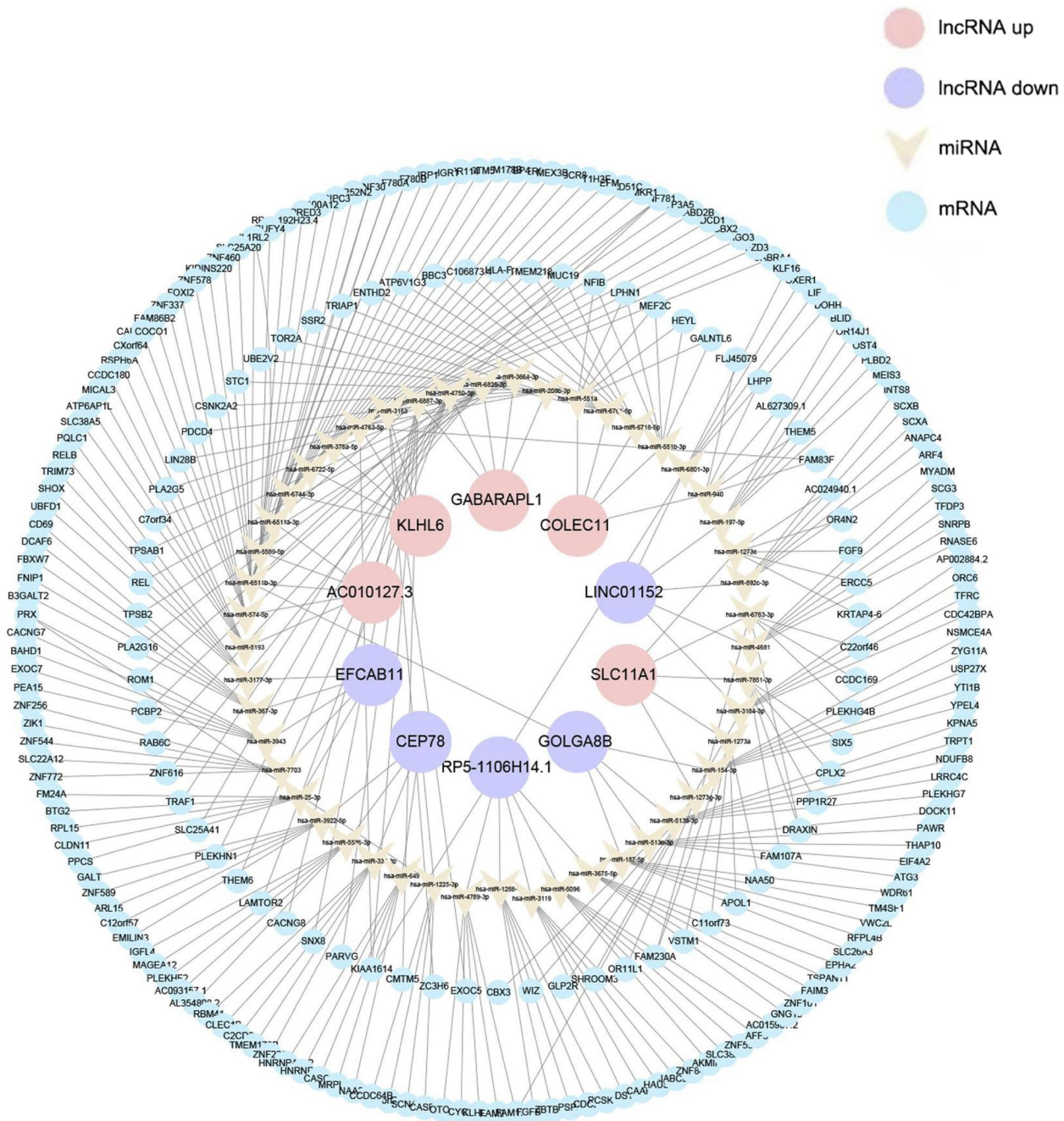

Fig. 5 The lncRNA–miRNA–mRNA regulatory network in RIF. The pink circular nodes represent upregulated lncRNAs, the purple circular nodes represent downregulated lncRNAs, the yellow triangular nodes represent miRNAs and the blue circular nodes represent mRNAs

confirmed that lncRNA hypomethylation can promote cancer cell cycle progression [50]. Consistently, a recent review suggested that m^6A methylation can promote cancer progression [51]. According to our GO analysis, the hypomethylated lncRNAs are mostly related to the cell cycle, implying that changes in m^6A methylation affect cell proliferation in patients with RIF.

The genes associated with hypomethylated lncRNAs are mainly involved in immunological processes, including NK cell–mediated cytotoxicity and the chemokine signalling pathway (Fig. 3D). The ability to kill other cells is an important effector mechanism of the immune system; NK cells are the major mediators of this activity [52]. NK cells are recruited and activated by ovarian

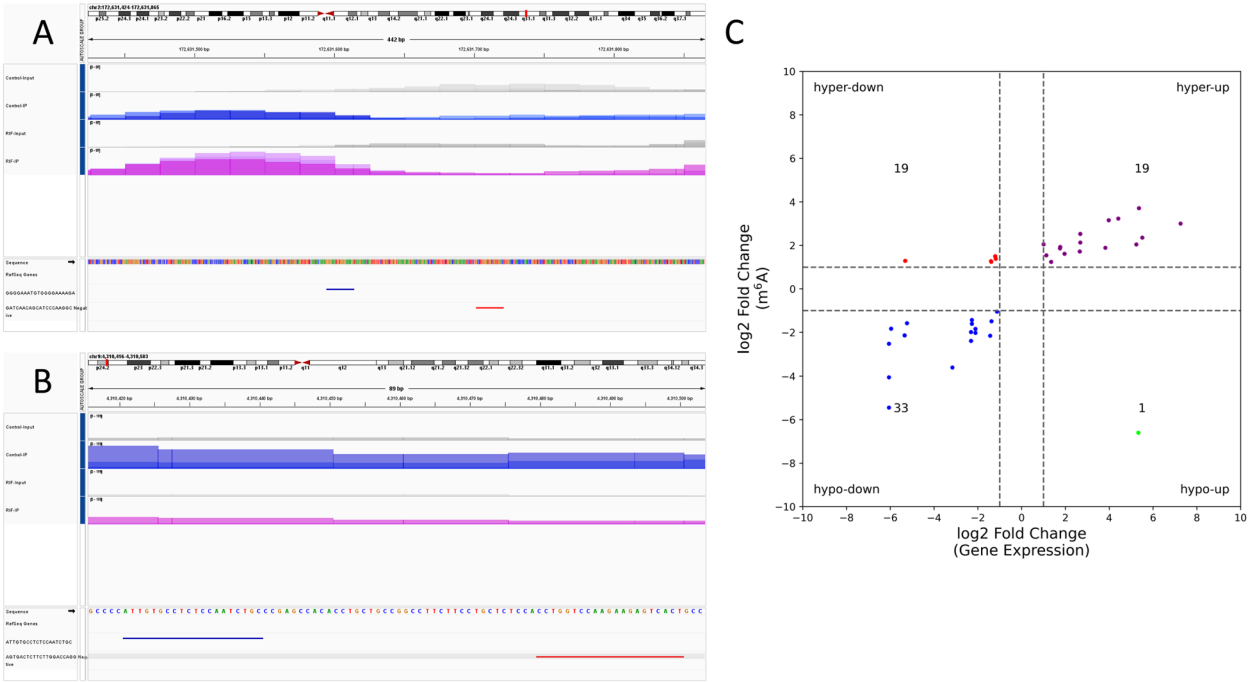

Fig. 6 Validation of the m^{6}A methylation abundances of lncRNAs. IGV plots of (**A**) ENST00000416361 and (**B**) ENST00000471664 m^{6}A methylation and expression abundances in the RIF and control groups. Each plot shows the MeRIP-qPCR primer binding regions. At the bottom of the IGV plot, blue and red represent primer positions and the middle region is the pcr product region. IP refers to the methylation level, and input refers to the expression level. **C** The four-quadrant plot shows the inclusion of differentially methylated DEGs(Differentially Expressed Genes) for m^{6}A peaks

hormones and play pivotal roles throughout pregnancy. Decidual natural killer (dNK) cells release chemokines that induce trophoblast invasion, tissue remodelling, embryonic development and placentation. NK cells can also mediate cytotoxicity and carry out immune defence in case of an in utero infection [53–55]. Researchers have suggested an association between RIF and abnormally elevated uterine NK cell levels and cytotoxicity [54]. It has been proposed that intrauterine administration of peripheral blood mononuclear cells (PBMCs) modulates the maternal immune response through a cascade of chemokines to favour implantation. This therapy could significantly improve the clinical pregnancy rate, a finding confirmed with a meta-analysis [56, 57]. Based on our results, we hypothesise that m^{6}A methylation associated with immunological processes influences the pregnancy outcome in patients with RIF.

Genes associated with hypomethylated lncRNAs are also involved in the p53 signalling pathway. p53 is a well-known tumour suppressor, but little is known about its other functions. With the aid of the p53MH algorithm, researchers identified *LIF* as a p53-regulated gene [58]. p53 is crucial for embryonic implantation through upregulation of uterine *LIF* transcription [59]. Recently, it has been proposed that the absence of PARP-1 and PARP-2 increases p53 signalling and the population of senescent decidual cells [60]. In a case–control survey with 100 patients with RIF and 100 normal pregnancies, the researchers suggested that p53 gene polymorphisms could be a genetic predisposing factor for RIF [61]. Based on the results of our study, m^{6}A might participate in the p53 signalling pathway and contribute to the pathogenic mechanism of RIF.

We constructed a ceRNA network to analyse the regulatory relationship between lncRNAs, miRNAs and mRNAs (Fig. 4). The potential target genes of several lncRNAs in this ceRNA are related to reproductive disease. For example, *LINC01152* could act as a sponge for hsa-miR-6801-3p to affect *LIF* expression (Fig. 4). *LIF* activates signal transducer and activator of transcription 3 (*STAT3*) precursors via uterine LIF receptors, allowing successful blastocyst implantation [62]. In addition to *LIF*, *PRX*, *CD69* and *HLA-F* are potential target genes in the ceRNA network. The expression of the *PRX* is significantly decreased in ectopic endometrium compared with eutopic or control endometrium [63]. In an endometrial immune assessment, the sub-fertile population exhibited increased *CD69* activation [64]. *HLA-F* fluctuates during

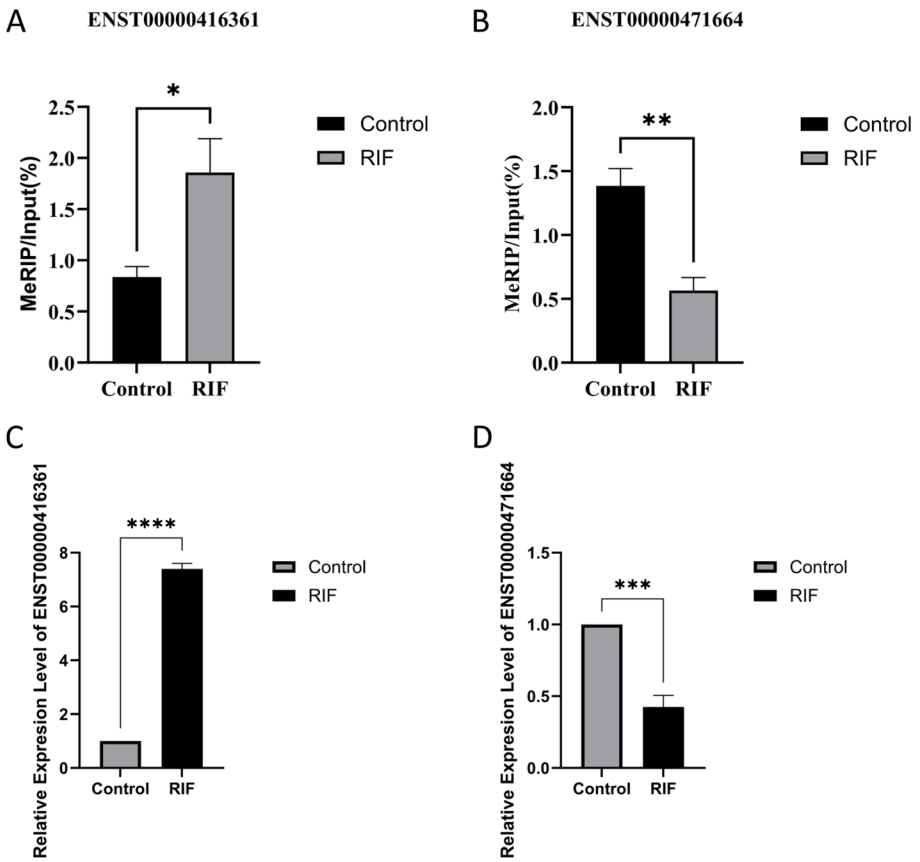

Fig. 7 The m^{6}A methylation abundances of (**A**) ENST00000416361 and (**B**) ENST00000471664 was validated in endometrial tissue with MeRIP-qPCR. The relative mRNA expression of (**C**) ENST00000416361 and (**D**) ENST00000471664 in endometrial tissue from the RIF group and Control group was determined with RT-qPCR. Statistical significance was determined using Student's *t*-test (*$P < 0.05$, **$P < 0.01$, ***$P < 0.001$, ****$p < 0.0001$)

the menstrual cycle, with high levels during the implantation window. HLA-F protein expression correlates with the number of CD56-positive NK cells in the mid-secretory endometrium [65]. The functions of abovementioned genes in decidualisation and RIF require further investigation. However, it is clear that the network provides insights to further understand the role of lncRNAs in the occurrence and development of RIF.

We verified the m^{6}A methylation abundance of three lncRNAs (ENST00000416361 and ENST00000471664) by using MeRIP-qPCR. ENST00000416361 is upregulated in coronary artery disease and is related to inflammation and lipid metabolism [66]. ENST00000471664 plays a significant role in GLIS3 knockout mouse pancreatic islets [67]. However, these studies are limited to bioinformatics. There have been many studies on the involvement of m^{6}A methylation in the expression of lncRNAs [68, 69]. We suspect that this process might influence lncRNA expression in RIF, although this speculation requires further investigation.

There are several limitations to our study. First, we only used a small number of samples. To make up for this deficiency, we used MeRIP-qPCR to ensure the accuracy of our m^{6}A-seq results. Second, we performed a descriptive bioinformatics analysis. It is necessary to explore the relationship of m^{6}A and lncRNAs in RIF in subsequent experiments.

Conclusions

In summary, we revealed the m^{6}A lncRNA methylation landscape by using high-throughput sequencing;. This endeavour has provided new perspectives on the pivotal roles of epigenetic changes in RIF. We generated a ceRNA network that demonstrated a regulatory relationship between lncRNAs, miRNAs and mRNAs. Additional experiments should be carried out to verify the differential methylated lncRNAs in patients with RIF.

Supplementary Information

The online version contains supplementary material available at https://doi.org/10.1186/s12920-024-02013-3.

Supplementary Material 1.

Supplementary Material 2.

Supplementary Material 3.

Acknowledgements
None.

Authors' contributions
The first two authors contributed equally to this work. Lin Liu designed and supervised the study. Ting Wang conducted the experiments and drafted the manuscript. Lili Zhang and Xiaoling Ma collected the samples. Wenxin Gao and Yidan Liu contributed the methodology. Feng Yue modified the format. All authors have read and approved the manuscript.

Funding
This work was financially supported by the National Natural Science Foundation of China (82360307), the Talent Innovation and Entrepreneurship Project of Lanzhou City (2022-RC-47), Gansu Provincial Science and Technology Program (20JR10TA715,21JR7RA391), the Medical Innovation and Development Project of Lanzhou University (lzuyxcx-2022–191), Science and Technology Project of Lanzhou (2023-ZD-93), Fund of the First Hospital of Lanzhou University (ldyyyn2022-60), Key Research and Development Plan of Gansu Province in 2022 (grant no. 22YF7FA084), Fund of the First Hospital of Lanzhou University (ldyyyn2019-86).

Data availability
No datasets were generated or analysed during the current study.

Declarations

Ethics approval and consent to participate
The study was approved by the Ethics Committee of Lanzhou University First Affiliated Hospital on 21/2/2019.
All procedures were in accordance with the ethical standards of the institutional research committee and with the Helsinki declaration and its later amendments or comparable ethical standards. Written informed consents were obtained from all patients prior to study commencement.

Consent for publication
Not applicable.

Competing interests
The authors declare no competing interests.

Received: 11 June 2024 Accepted: 17 September 2024
Published online: 11 October 2024

References

1. Coughlan C, Ledger W, Wang Q, Liu F, Demirol A, Gurgan T, et al. Recurrent implantation failure: definition and management. Reprod Biomed Online. 2014;28(1):14–38.
2. Mrozikiewicz AE, Ożarowski M, Jędrzejczak P. Biomolecular markers of recurrent implantation failure-a review. Int J Mol Sci. 2021;22(18):10082.
3. Ochoa-Bernal MA, Fazleabas AT. Physiologic events of embryo implantation and decidualization in human and non-human primates. Int J Mol Sci. 2020;21(6):1973.
4. Quinn KE, Matson BC, Wetendorf M, Caron KM. Pinopodes: ecent advancements, current perspectives, and future directions. Mol Cell Endocrinol. 2020;501:110644.
5. Bastu E, Mutlu MF, Yasa C, Dural O, Nehir Aytan A, Celik C, et al. Role of Mucin 1 and glycodelin A in recurrent implantation failure. Fertil Steril. 2015;103(4):1059-64 e2.
6. Wu F, Chen X, Liu Y, Liang B, Xu H, Li TC, Wang CC. Decreased MUC1 in endometrium is an independent receptivity marker in recurrent implantation failure during implantation window. Reprod Biol Endocrinol. 2018;16(1):60.
7. Zhu M, Yi S, Huang X, Meng J, Sun H, Zhou J. Human chorionic gonadotropin improves endometrial receptivity by increasing the expression of homeobox A10. Mol Hum Reprod. 2020;26(6):413–24.
8. Wei CM, Gershowitz A, Moss B. Methylated nucleotides block 5' terminus of HeLa cell messenger RNA. Cell. 1975;4(4):379–86.
9. Liu ZX, Li LM, Sun HL, Liu SM. Link Between m6A modification and cancers. Front Bioeng Biotechnol. 2018;6:89.
10. Fang Z, Mei W, Qu C, Lu J, Shang L, Cao F, Li F. Role of m6A writers, erasers and readers in cancer. Exp Hematol Oncol. 2022;11(1):45.
11. He L, Li H, Wu A, Peng Y, Shu G, Yin G. Functions of N6-methyladenosine and its role in cancer. Mol Cancer. 2019;18(1):176.
12. Zhao S, Lu J, Chen Y, Wang Z, Cao J, Dong Y. Exploration of the potential roles of m6A regulators in the uterus in pregnancy and infertility. J Reprod Immunol. 2021;146:103341.
13. Xue P, Zhou W, Fan W, Jiang J, Kong C, Zhou W, et al. Increased METTL3-mediated m(6)A methylation inhibits embryo implantation by repressing HOXA10 expression in recurrent implantation failure. Reprod Biol Endocrinol. 2021;19(1):187.
14. Wang Y, Hu S, Yao G, Zhu Q, He Y, Lu Y, et al. A novel molecule in human cyclic endometrium: LncRNA TUNAR is involved in embryo implantation. Front Physiol. 2020;11:587448.
15. Feng C, Shen JM, Lv PP, Jin M, Wang LQ, Rao JP, Feng L. Construction of implantation failure related lncRNA-mRNA network and identification of lncRNA biomarkers for predicting endometrial receptivity. Int J Biol Sci. 2018;14(10):1361–77.
16. Pan T. N6-methyl-adenosine modification in messenger and long non-coding RNA. Trends Biochem Sci. 2013;38(4):204–9.
17. Coker H, Wei G, Brockdorff N. m6A modification of non-coding RNA and the control of mammalian gene expression. Biochim Biophys Acta. 2019;1862(3):310–8.
18. Deng K, Ning X, Ren X, Yang B, Li J, Cao J, et al. Transcriptome-wide N6-methyladenosine methylation landscape of coronary artery disease. Epigenomics. 2021;13(10):793–808.
19. Lv Z, Sun L, Xu Q, Xing C, Yuan Y. Joint analysis of lncRNA m(6)A methylome and lncRNA/mRNA expression profiles in gastric cancer. Cancer Cell Int. 2020;20:464.
20. Niu X, Xu J, Liu J, Chen L, Qiao X, Zhong M. Landscape of N(6)-Methyladenosine modification patterns in human Ameloblastoma. Front Oncol. 2020;10:556497.
21. Wu J, Deng LJ, Xia YR, Leng RX, Fan YG, Pan HF, Ye DQ. Involvement of N6-methyladenosine modifications of long noncoding RNAs in systemic lupus erythematosus. Mol Immunol. 2022;143:77–84.
22. Xu Z, Tian P, Guo J, Mi C, Liang T, Xie J, et al. Lnc-HZ01 with m6A RNA methylation inhibits human trophoblast cell proliferation and induces miscarriage by up-regulating BPDE-activated lnc-HZ01/MXD1 positive feedback loop. Sci Total Environ. 2021;776:145950.
23. Martin M. Cutadapt removes adapter sequences from high-throughput sequencing reads. Embnet J. 2011;17(1):10–2.
24. Kim D, Langmead B, Salzberg SL. HISAT: a fast spliced aligner with low memory requirements. Nat Methods. 2015;12(4):357–60.
25. Anders S, Pyl PT, Huber W. HTSeq–a Python framework to work with high-throughput sequencing data. Bioinformatics (Oxford, England). 2015;31(2):166–9.
26. Robinson MD, McCarthy DJ, Smyth GK. edgeR: a Bioconductor package for differential expression analysis of digital gene expression data. Bioinformatics (Oxford, England). 2010;26(1):139–40.
27. Zhang Y, Liu T, Meyer CA, Eeckhoute J, Johnson DS, Bernstein BE, et al. Model-based analysis of ChIP-Seq (MACS). Genome Biol. 2008;9(9):R137.
28. Shen L, Shao NY, Liu X, Maze I, Feng J, Nestler EJ. diffReps: detecting differential chromatin modification sites from ChIP-seq data with biological replicates. PLoS One. 2013;8(6):e65598.
29. Kanehisa M, Furumichi M, Sato Y, Kawashima M, Ishiguro-Watanabe M. KEGG for taxonomy-based analysis of pathways and genomes. Nucleic Acids Res. 2022;51(D1):D587-92.

30. Miao YR, Liu W, Zhang Q, Guo AY. lncRNASNP2: an updated database of functional SNPs and mutations in human and mouse lncRNAs. Nucleic Acids Res. 2018;46(D1):D276–80.
31. Smoot ME, Ono K, Ruscheinski J, Wang PL, Ideker T. Cytoscape 2.8: new features for data integration and network visualization. Bioinformatics (Oxford, England). 2011;27(3):431–2.
32. Agarwal V, Bell GW, Nam JW, Bartel DP. Predicting effective microRNA target sites in mammalian mRNAs. eLife. 2015;4:e05005.
33. Bailey TL. DREME: motif discovery in transcription factor ChIP-seq data. Bioinformatics (Oxford, England). 2011;27(12):1653–9.
34. Ponting CP, Oliver PL, Reik W. Evolution and functions of long noncoding RNAs. Cell. 2009;136(4):629–41.
35. Laboratories K. KEGG Copyright Permission 2022 [Available from: https://www.kegg.jp/kegg/kegg1.html.
36. Xu M, Zhou C, Weng J, Chen Z, Zhou Q, Gao J, et al. Tumor associated macrophages-derived exosomes facilitate hepatocellular carcinoma malignance by transferring lncMMPA to tumor cells and activating glycolysis pathway. J Exp Clin Cancer Res. 2022;41(1):253.
37. Zheng G, Dahl JA, Niu Y, Fedorcsak P, Huang CM, Li CJ, et al. ALKBH5 is a mammalian RNA demethylase that impacts RNA metabolism and mouse fertility. Mol Cell. 2013;49(1):18–29.
38. Li X, Xiong W, Long X, Dai X, Peng Y, Xu Y, et al. Inhibition of METTL3/m6A/miR126 promotes the migration and invasion of endometrial stromal cells in endometriosis†. Biol Reprod. 2021;105(5):1221–33.
39. Zou J, Li Y, Liao N, Liu J, Zhang Q, Luo M, et al. Identification of key genes associated with polycystic ovary syndrome (PCOS) and ovarian cancer using an integrated bioinformatics analysis. J Ovarian Res. 2022;15(1):30.
40. McGlacken-Byrne SM, Del Valle I, Quesne Stabej PL, Bellutti L, Garcia-Alonso L, Ocaka LA, et al. Pathogenic variants in the human m6A reader YTHDC2 are associated with primary ovarian insufficiency. JCI Insight. 2022;7(5):e154671.
41. Taylor HS. The role of HOX genes in human implantation. Hum Reprod Update. 2000;6(1):75–9.
42. Zhao H, Hu S, Qi J, Wang Y, Ding Y, Zhu Q, et al. Increased expression of HOXA11-AS attenuates endometrial decidualization in recurrent implantation failure patients. Mol Ther. 2022;30(4):1706–20.
43. Zhao F, Chen T, Zhao X, Wang Q, Lan Y, Liang Y, et al. LINC02190 inhibits the embryo-endometrial attachment by decreasing ITGAD expression. Reproduction (Cambridge, England). 2022;163(2):107–18.
44. Zuo L, Su H, Zhang Q, Wu WY, Zeng Y, Li XM, et al. Comprehensive analysis of lncRNAs N(6)-methyladenosine modification in colorectal cancer. Aging. 2021;13(3):4182–98.
45. May-Dracka TL, Gao F, Hopkins BT, Hronowski X, Chen T, Chodaparambil JV, et al. Discovery of phospholipase D inhibitors with improved drug-like properties and central nervous system penetrance. ACS Med Chem Lett. 2022;13(4):665–73.
46. Bekdash RA. Neuroprotective effects of choline and other methyl donors. Nutrients. 2019;11(12):2995.
47. Yurci A, Dokuzeylul Gungor N, Gurbuz T. Spectroscopy analysis of endometrial metabolites is a powerful predictor of success of embryo transfer in women with implantation failure: a preliminary study. Gynecol Endocrinol. 2021;37(5):415–21.
48. RoyChoudhury S, Singh A, Gupta NJ, Srivastava S, Joshi MV, Chakravarty B, Chaudhury K. Repeated implantation failure versus repeated implantation success: discrimination at a metabolomic level. Hum Reprod. 2016;31(6):1265–74.
49. Zhang Y, Zhang T, Wu L, Li TC, Wang CC, Chung JPW. Metabolomic markers of biological fluid in women with reproductive failure: a systematic review of current literatures. Biol Reprod. 2022;106:1049.
50. Wang Z, Yang B, Zhang M, Guo W, Wu Z, Wang Y, et al. lncRNA epigenetic landscape analysis identifies EPIC1 as an oncogenic lncRNA that interacts with MYC and promotes cell-cycle progression in cancer. Cancer Cell. 2018;33(4):706-20.e9.
51. Sun H, Li K, Liu C, Yi C. Regulation and functions of non-m(6)A mRNA modifications. Nat Rev Mol Cell Biol. 2023;24(10):714–31.
52. Prager I, Watzl C. Mechanisms of natural killer cell-mediated cellular cytotoxicity. J Leukoc Biol. 2019;105(6):1319–29.
53. Díaz-Hernández I, Alecsandru D, García-Velasco JA, Domínguez F. Uterine natural killer cells: from foe to friend in reproduction. Hum Reprod Update. 2021;27(4):720–46.
54. Sfakianoudis K, Rapani A, Grigoriadis S, Pantou A, Maziotis E, Kokkini G, et al. The role of uterine natural killer cells on recurrent miscarriage and recurrent implantation failure: from pathophysiology to treatment. Biomedicines. 2021;9(10):1425.
55. Zhang X, Wei H. Role of decidual natural killer cells in human pregnancy and related pregnancy complications. Front Immunol. 2021;12:728291.
56. Yakin K, Oktem O, Urman B. Intrauterine administration of peripheral mononuclear cells in recurrent implantation failure: a systematic review and meta-analysis. Sci Rep. 2019;9(1):3897.
57. Yang DN, Wu JH, Geng L, Cao LJ, Zhang QJ, Luo JQ, et al. Efficacy of intrauterine perfusion of peripheral blood mononuclear cells (PBMC) for infertile women before embryo transfer: meta-analysis. J Obstet Gynaecol. 2020;40(7):961–8.
58. Hu W, Feng Z. The role of p53 in reproduction, an unexpected function for a tumor suppressor. J Mol Cell Biol. 2019;11(7):624–7.
59. Levine AJ, Tomasini R, McKeon FD, Mak TW, Melino G. The p53 family: guardians of maternal reproduction. Nat Rev Mol Cell Biol. 2011;12(4):259–65.
60. Kelleher AM, Setlem R, Dantzer F, DeMayo FJ, Lydon JP, Kraus WL. Deficiency of PARP-1 and PARP-2 in the mouse uterus results in decidualization failure and pregnancy loss. Proc Natl Acad Sci U S A. 2021;118(40):e2109252118.
61. Mohammadzadeh M, Ghorbian S, Nouri M. Evaluation of clinical utility of P53 gene variations in repeated implantation failure. Mol Biol Rep. 2019;46(3):2885–91.
62. Fukui Y, Hirota Y, Saito-Fujita T, Aikawa S, Hiraoka T, Kaku T, et al. Uterine epithelial LIF receptors contribute to implantation chamber formation in blastocyst attachment. Endocrinology. 2021;162(11):bqab169.
63. Yu H, Hao JM, Li X, Li F, Li J, Li L. Decreased expression of peroxiredoxin in patients with ovarian Endometriosis Cysts. Arch Med Res. 2020;51(7):670–4.
64. Marron K, Walsh D, Harrity C. Detailed endometrial immune assessment of both normal and adverse reproductive outcome populations. J Assist Reprod Genet. 2019;36(2):199–210.
65. Nilsson LL, Hviid TVF. HLA Class Ib-receptor interactions during embryo implantation and early pregnancy. Hum Reprod Update. 2022;28(3):435–54.
66. Li P, Yan X, Xu G, Pang Z, Weng J, Yin J, et al. A novel plasma lncRNA ENST00000416361 is upregulated in coronary artery disease and is related to inflammation and lipid metabolism. Mol Med Rep. 2020;21(6):2375–84.
67. Scoville DW, Gruzdev A, Jetten AM. Identification of a novel lncRNA (G3R1) regulated by GLIS3 in pancreatic β-cells. J Mol Endocrinol. 2020;65(3):59–67.
68. Zhang L, Wan Y, Zhang Z, Jiang Y, Gu Z, Ma X, et al. IGF2BP1 overexpression stabilizes PEG10 mRNA in an m6A-dependent manner and promotes endometrial cancer progression. Theranostics. 2021;11(3):1100–14.
69. Liu HT, Zou YX, Zhu WJ, Sen L, Zhang GH, Ma RR, et al. lncRNA THAP7-AS1, transcriptionally activated by SP1 and post-transcriptionally stabilized by METTL3-mediated m6A modification, exerts oncogenic properties by improving CUL4B entry into the nucleus. Cell Death Differ. 2022;29(3):627–41.

Publisher's Note